Contribution from the School of Science,
University of Waikato, Hamilton, New Zealand

Characterization of Open Clusters with Linked $GeFe_2$ or $SnFe_2$ Triangles: Structures of $Ge_2Fe_6(CO)_{23}$, $Sn_2Fe_6(CO)_{23}$, and $Ge_2Fe_7(CO)_{26}$

Skelte G. Anema, Kenneth M. Mackay,* and Brian K. Nicholson*

Received January 20, 1989

Reactions of GeH_4 or Ge_2H_6 with $Fe_2(CO)_9$ in hexane at 68 °C have revealed a rich system. Two new Ge–Fe clusters have been spectroscopically and structurally characterized; $Ge_2Fe_6(CO)_{23}$ (**3b**) is the linked-triangle homologue of $Ge[Fe_2(CO)_8]_2$ with four $GeFe_2$ units [$C_{23}Fe_6Ge_2O_{23}$, a = 13.872 (1) Å, b = 14.5501 (7) Å, c = 9.2221 (7) Å, α = 96.875 (6)°, β = 97.152 (6)°, γ = 67.398 (6)°, triclinic, $P\bar{1}$, Z = 2], while $Ge_2Fe_7(CO)_{26}$ (**4b**) shows two μ-$Ge[Fe_2(CO)_8]$ groups on adjacent sides of an Fe_3 triangle [$C_{26}Fe_7Ge_2O_{26}$, a = 17.25 (1) Å, b = 17.14 (1) Å, c = 25.89 (4) Å, orthorhombic, $Pbca$, Z = 8]. The analogous tin complexes are formed with use of SnH_4, and $Sn_2Fe_6(CO)_{23}$ (**3a**) with four $SnFe_2$ triangles has been structurally characterized [$C_{23}Fe_6Sn_2O_{23}$, a = 8.921 (1) Å, b = 12.551 (3) Å, c = 16.444 (5) Å, α = 95.65 (2)°, β = 104.53 (2)°, γ = 100.83 (2)°, triclinic, $P\bar{1}$, Z = 2].

Introduction

In a pioneering study in 1967, Stone and his colleagues[1] showed that heating Bu_3SnCl, Me_3SnH, or Me_2SnH_2 with $Fe(CO)_5$ formed a number of compounds containing Sn–Fe bonds, including clusters based on three-membered $SnFe_2$ or four-membered Sn_2Fe_2 rings. The crystal structure of one of these, $Sn[Fe_2(CO)_8]_2$ (**1a**), was determined.[2] Later, the corresponding Ge[3-6] (**1b**) and Pb[6] (**1c**) species were reported.

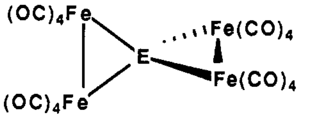

1a. E = Sn
1b. E = Ge
1c. E = Pb
1d. E = Si

We have recently[7] prepared the silicon analogue $Si[Fe_2(CO)_8]_2$ (**1d**) by the reaction of SiH_4 with $Fe_2(CO)_9$ and studied the corresponding reaction of GeH_4 to improve the yield of $Ge[Fe_2(CO)_8]_2$ (**1b**). These compounds all form part of the larger field of "naked" main-group-atom metal complexes so stimulatingly reviewed by Herrmann.[8]

The reaction of GeH_4 with $Fe_2(CO)_9$ was more complex than the corresponding one with silane, giving[7] a minor product and several trace products in addition to **1b**. A similar reaction of SnH_4 with $Fe_2(CO)_9$ gave rise to an even wider range of clusters,[9] including **1a**, and the new cluster $SnFe_5(CO)_{19}$ (**2a**) with a structure related to that of $Fe_3(CO)_{12}$. Two other species were present in modest yields but were not fully separated, and additional trace components were also seen.

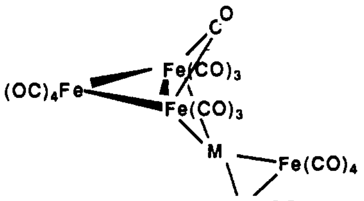

2a. M = Sn
2b. M = Ge

These reactions of GeH_4 and SnH_4 with $Fe_2(CO)_9$ compare interestingly with the reactions[6] of divalent Ge or Sn compounds with $[Fe_2(CO)_8]^{2-}$, which yielded the new clusters $[GeFe_4(CO)_{14}]^{2-}$ and $[Sn\{Fe_2(CO)_8\}\{Fe(CO)_4\}_2]^{2-}$, respectively. These compounds could be oxidized to **1b** or **1a**.

We now report the separation of the mixed tin species and their identification as $Sn_2Fe_6(CO)_{23}$ (**3a**) and $Sn_2Fe_7(CO)_{26}$ (**4a**). We have also extended the study of the germanium system by examining the reaction of Ge_2H_6 with $Fe_2(CO)_9$. This gave no new products but increased yields of several. Thus, the minor product of the GeH_4 reaction was shown to be **3b**, and two of the trace components were shown to be **4b** and, probably, **2b**, the analogue of the characterized tin compound **2a**. In this paper we describe full details of these reactions, together with the crystallographic characterization of three of the new clusters, **3a**, **3b**, and **4b**. The corresponding reaction of Si_2H_6 with $Fe_2(CO)_9$ has also been examined.

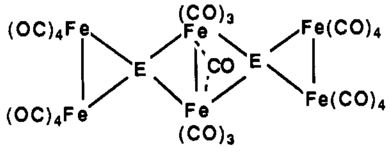

3a. E = Sn
3b. E = Ge

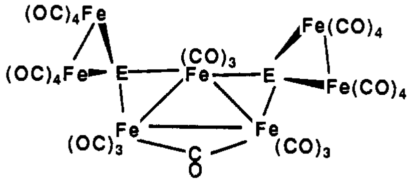

4a. E = Sn
4b. E = Ge

Experimental Section

General Methods. Handling, radial chromatography, and hydride preparation used the methods reported earlier.[7,9] Ge_2H_6 was a coproduct with germane,[10] and Si_2H_6 was formed by $LiAlH_4$ reduction of the chloride. Infrared spectra were recorded on a Perkin-Elmer 180 spectrometer and Raman data on a Spex Ramalog 1403 spectrometer using a Spectra-Physics 25-mW He-Ne laser, while mass spectra were recorded on a Varian CH5 machine.

Reaction of GeH_4 with $Fe_2(CO)_9$. This reaction was carried out as previously described,[7] but at 68 °C, to give a mixture of products. Preparative chromatography on silica, with petroleum spirit/dichloromethane (1:1) eluent, gave, in order of elution, green $Fe_3(CO)_{12}$ (ca. 5%), yellow **1b** (35–45%, characterized spectroscopically[4,5]), an unidentified orange minor product (<1%), brown-green $Ge_2Fe_7(CO)_{26}$ (**4b**; 1–2%, see below for characterization), orange $Ge_2Fe_6(CO)_{23}$ (**3b**; ca. 7%, see below for characterization), an unidentified green component (<1%), which may be $GeFe_5(CO)_{19}$ (cf. **2a**), and a red-brown uneluted immobile band.

The reaction conditions are critical; above 70 °C $Fe_3(CO)_{12}$ is rapidly formed, while at temperatures below 65 °C yields of **1b** and **3b** decrease,

---

(1) Cotton, J. D.; Knox, S. A. R.; Paul, I.; Stone, F. G. A. *J. Chem. Soc. A* **1967**, 264.
(2) Lindley, P. F.; Woodward, P. *J. Chem. Soc. A* **1967**, 382.
(3) Cotton, J. D.; Peachey, R. M. *Inorg. Nucl. Chem. Lett.* **1970**, *6*, 727.
(4) Batsanov, A. S.; Rybin, L. V.; Rybinskaya, M. I.; Struchkov, Y. T.; Salimgareeva, I. M.; Bogatova, N. G. *J. Organomet. Chem.* **1983**, *249*, 319.
(5) Melzer, D.; Weiss, E. *J. Organomet. Chem.* **1983**, *255*, 335.
(6) Whitmire, K. H.; Lagrone, C. B.; Churchill, M. R.; Fettinger, J. C.; Robinson, B. H. *Inorg. Chem.* **1987**, *26*, 3491.
(7) Anema, S. G.; Barris, G. C.; Mackay, K. M.; Nicholson, B. K. *J. Organomet. Chem.* **1988**, *350*, 207.
(8) Herrmann, W. A. *Angew. Chem., Int. Ed. Engl.* **1986**, *25*, 56.
(9) Anema, S. G.; Mackay, K. M.; Nicholson, B. K. *J. Organomet. Chem.*, in press.
(10) Jolly, W.; Drake, J. E. *Inorg. Synth.* **1963**, *7*, 35.

0020-1669/89/1328-3158$01.50/0 © 1989 American Chemical Society

the major product being a red compound, soluble in CH_2Cl_2, which was very unstable. This showed CO stretches at (cm^{-1}) 2095 vw, 2064 mw, 2019 vs, 1991 vs, 1960 vw, br, sh, and 1830 w br but could not be identified. **4b** was formed only in the 68 °C reactions.

To check whether the byproduct $Fe_3(CO)_{12}$ acts as an intermediate, a similar reaction was carried out between GeH_4 and $Fe_3(CO)_{12}$. There was no reaction below 50 °C. Reaction at 68 °C gave **1b** (5%), while the major product was a red species, different from that formed from $Fe_2(CO)_9$ as it was insoluble in dichloromethane, and was not further examined. A similar test reaction with $Fe(CO)_5$ showed no reaction with GeH_4 under these conditions up to 70 °C.

Reaction of Ge_2H_6 with $Fe_2(CO)_9$. A mixture of $Fe_2(CO)_9$ (830 mg, 2.27 mmol), Ge_2H_6 (0.31 mmol), and pentane (50 mL) was sealed in a 200-mL ampule fitted with a greaseless tap and heated to 68 °C for 15 min. The initially colorless solution changed through yellow to red-brown to dark brown. The tube was opened, and noncondensable gases were measured at the Toepler pump (0.86 mmol total, 0.73 mmol of H_2, 0.13 mmol of CO). The solvent (containing $Fe(CO)_5$ and some unreacted Ge_2H_6) was pumped off. The residue was chromatographed on silica plates, with hexane/dichloromethane (2:1) eluent, to give the following in order of elution: green $Fe_3(CO)_{12}$ (R_f 0.86; trace), yellow $Ge[Fe_2(CO)_8]_2$ (**1b**; R_f 0.77; 87 mg, 0.12 mmol, 19% based on Ge), brown $Ge_2Fe_7(CO)_{26}$ (**4b**; R_f 0.72; 77 mg, 0.060 mmol, 20%), and orange $Ge_2Fe_6(CO)_{23}$ (**3b**; R_f 0.69; 83 mg, 0.074 mmol, 24%), all identified by infrared spectroscopy. **3b** and **4b** were clearly decomposing during the chromatography, so these yields underestimate the conversion. Modest variations in reaction ratio and reaction time did not significantly alter the overall or relative yields of **1b**, **3b**, and **4b**. When a similar reaction was run at room temperature, it took 20 days for the color to darken substantially. The major product was the same unstable soluble red species as found[7] in the lower temperature GeH_4 reactions. The identified products were **1b** (5%) and **3b** (4.5%). No **4b** was detectable.

Characterization of $Ge_2Fe_6(CO)_{23}$. **3b** forms bright orange crystals, reasonably stable in air as a solid, but the compound is oxidized in solution. Electron probe analysis gave a Ge:Fe ratio of 1.0:3.2. No mass spectrum could be recorded, presumably because of a lack of volatility at probe temperatures below the decomposition temperature. IR spectra (cm^{-1}; ν(CO)): 2090 m, 2054 vs, 2037 vs, 1994 m, 1965 sh, 1827 w (in CH_2Cl_2) [cf. $Sb_2Fe_6(CO)_{22}$,[11] 2090 m, 2060 m, 2038 s, 1995 w, 1960 w]; 2108 w, 2089 s, 2061 sh, 2054 sh, 2040 sh, 2030 vvs, 2019 sh, 2003 vw, 2000 mw, 1985 vs, 1981 vs, 1966 w, 1826 s, 660 sh, 653 vs, 627 vw, 618 vs, 518 s, br, 278 w, 246 w (as CsCl disk). Raman shifts (cm^{-1}, solid): 2110 s, 2095 vw, 2068 vw, 2058 w, 2048 w, 2034 s, 2020 w, 2006 vs, 1993 w, 1987 m, 640 vw, 534 vw, 485 w, 456 s, 395 w, br, 288 w, 232 s, 202 sh, 181 s, 140–80 vs, br.

The compound was further characterized by a single-crystal X-ray analysis (see below).

Characterization of $Ge_2Fe_7(CO)_{26}$. **4b** is a stable dark brown solid, dissolving in polar organic solvents to give deep red solutions. Electron probe analysis gave a Ge:Fe ratio of 2.0:7.2. A mass spectrum gave an envelope at *m/e* ca. 1130, at the limit of the spectrometer, which corresponds to $[P - 5\ CO]^+$, followed by peaks corresponding to loss of the remaining 21 carbonyl groups. In the IR spectrum ν(CO) modes were as follows (cm^{-1}): 2090 m, 2067 w, 2054 vs, 2034 s, 2015 s, 1970 w, 1858 w, br (in CH_2Cl_2); 2086 s, 2053 w, 2042 w, sh, 2040 vs, 2027 vs, 2020 br, sh, 2011 sh, 2004 mw, 1988 vw, 1978 vw, 1862 ms (solid). The color was too dark to yield a Raman spectrum. The compound was further characterized by a single-crystal X-ray analysis (see below).

Reaction of SnH_4 with $Fe_2(CO)_9$. The details of the reaction of SnH_4 with $Fe_2(CO)_9$ in hexane have been published elsewhere,[9] and the most mobile and least mobile fractions on chromatography were shown to be **1a** and **2a**, respectively.[9] Two intermediate products were not separated pure in the earlier study. These have now been isolated, albeit in low yields, by careful chromatography and fractional crystallization. The orange band, R_f 0.64, had Sn:Fe = 1.0:3.1 and showed CO stretches at 2088 m, 2053 vs, 2037 vs, 2015 m, 2002 m, 1963 sh, and 1825 vw cm^{-1} (infrared spectrum in CH_2Cl_2) assigned to **3a** by comparison with the spectrum of the germanium analogue above and confirmed by an X-ray single-crystal analysis (see below).

The brown band, R_f 0.68, was available only in sufficient amount to yield an IR spectrum in CH_2Cl_2 solution. This gave CO stretches (cm^{-1}) at 2088 s, 2065 w, 2050 vs, 2032 s, 2012 m, and 1970 w assigned to **4a** by comparison with the spectrum of the germanium analogue above.

Reaction of Si_2H_6 with $Fe_2(CO)_9$. $Fe_2(CO)_9$ (1.01 g, 2.77 mmol) and hexane (30 mL) were placed in a 200-mL ampule, and Si_2H_6 (0.33 mmol) was distilled in on the vacuum line. The ampule was sealed and heated at 68 °C for 15 min, and the mixture turned dark brown. When the ampule was opened, incondensable gases (1.15 mmol, CO:H_2 = 1:5) were removed. Pumping gave volatiles consisting of hexane, some unreacted Si_2H_6, and $Fe(CO)_5$. An infrared spectrum of a CH_2Cl_2 extract of the residue showed bands assignable to $Si[Fe_2(CO)_8]_2$ (**1d**) and $Fe_3(CO)_{12}$, together with an unidentified species. After chromatography **1d** was recovered pure (0.090 g, 28%) together with $Fe_3(CO)_{12}$ (not measured) and a red species that adhered to the plate. There was no indication of higher clusters analogous to those found in the germane and stannane systems.

Table I. Crystallographic Data for **3a**, **3b**, and **4b**

	3b	**3a**	**4b**
formula	$C_{23}Fe_6Ge_2O_{23}$	$C_{23}Fe_6Sn_2O_{23}$	$C_{26}Fe_7Ge_2O_{26}$
fw	1124.5	1216.7	1264.4
space group	$P\bar{1}$ (No. 2)	$P\bar{1}$ (No 2)	*Pbca* (No. 61)
a, Å	13.872 (1)	8.921 (1)	17.25 (1)
b, Å	14.5501 (7)	12.551 (3)	17.14 (1)
c, Å	9.2221 (7)	16.444 (5)	25.89 (4)
α, deg	96.875 (6)	95.65 (2)	90
β, deg	97.152 (6)	104.53 (2)	90
γ, deg	67.398 (6)	100.83 (2)	90
V, Å^3	1699.9 (2)	1730 (1)	7653 (14)
Z	2	2	8
T, °C	21	−90	−100
ρ_{calcd}, g cm^{-3}	2.19	2.35	2.19
μ, cm^{-1}	53	40	43
2θ range, deg	$2 < 2\theta < 53$	$2 < 2\theta < 45$	$2 < 2\theta < 38$
no. of obsd data	5514 [$>3\sigma(I)$]	1851 [$>3\sigma(I)$]	1820 [$>\sigma(I)$]
transmission factors (max, min)	0.99, 0.85	0.90, 0.61	0.95, 0.54
$R(F_o)$, $R_w(F_o)$	0.0372, 0.0411	0.0618, 0.0467	0.124, 0.088

A similar run at 30 °C required 20 days to turn fully brown. Workup yielded H_2 (0.80 mmol), CO (0.35 mmol), unreacted Si_2H_6, and $Fe(CO)_5$ in the solvent fraction, and chromatography gave **1d** (90 mg, 20%) together with $Fe_3(CO)_{12}$ and the red species retained on the plate.

X-ray Crystallography. Crystallographic details for the structures of **3a**, **3b**, and **4b** are given in Table I. For **4b** only very thin crystals could be obtained, leading to a structure less precise than usual. For each structure, preliminary precession photography was used to define the space group. Cell dimensions and intensity data were determined on a Nicolet P3 diffractometer using monochromated Mo Kα X-rays (λ = 0.7107 Å). Absorption corrections were empirical, based on ϕ scans, for **3a** and **3b** and numerical for **4b**. Structures were solved by direct methods (SHELXS-86[12]) routinely developed and refined by full-matrix least squares (SHELX-76[12]), with all atoms assigned anisotropic temperature factors for **3b** but with only the metal atoms treated anisotropically for **3a** and **4b**. Scattering factors, including anomolous dispersion, were from ref 13. Final positional parameters are given in Tables II–IV, while selected bond lengths and angles are given in Tables V–VII. Full lists of bond angles, temperature factors, and structure factors have been deposited as supplementary material.

Results and Discussion

Preparations. The earlier work[7] on the reaction of GeH_4 with $Fe_2(CO)_9$, with temperatures of 65 °C and reaction times of 15 min, gave $Ge[Fe_2(CO)_8]_2$ (**1b**) as the main identified product, together with about 10% of the compound now identified as $Ge_2Fe_6(CO)_{23}$ (**3b**) and minor unidentified species. Raising the temperature slightly to 68 °C gives similar yields of **1b** and **3b** but produces a third product, shown to be $Ge_2Fe_7(CO)_{26}$ (**4b**), in sufficient amount to allow its isolation. In addition, there resulted a small amount of a fourth product, which is very tentatively suggested to be $GeFe_5(CO)_{19}$ (**2b**) from its color and chromatographic characteristics, which are similar to those of $SnFe_5(CO)_{19}$ (**2a**).

The recognition that **3b** and **4b** were digermanium species suggested that increased quantities may be available by starting from Ge_2H_6, from comparisons with the analogous cobalt carbonyl system.[14,15] This turned out to be the case. In the reaction of

---

(11) Arif, A. M.; Cowley, A. H.; Pakulski, M. *J. Chem. Soc., Chem. Commun.* **1987**, 623. Rheingold, A. L.; Geib, S. J.; Shieh, M.; Whitmire, K. H. *Inorg. Chem.* **19887**, *26*, 463.

(12) Sheldrick, G. M. "SHELX76, Program for Crystal Structure Determination"; University of Cambridge: Cambridge, England, Gottingen, FRG, 1986.

(13) *International Tables for X-ray Crystallography*; Kynoch: Birmingham, England, 1974; Vol. 4.

(14) Foster, S. P.; Mackay, K. M.; Nicholson, B. K. *Inorg. Chem.* **1985**, *24*, 909.

(15) Anema, S. G.; Mackay, K. M.; McLeod, L. C.; Nicholson, B. K.; Whittaker, J. M. *Angew. Chem., Int. Ed. Engl.* **1986**, *25*, 759.

Table II. Final Positional Parameters for $Ge_2Fe_6(CO)_{23}$ (**3b**)

atom	*x*	*y*	*z*	atom	*x*	*y*	*z*
Ge(1)	0.8548 (1)	0.2811 (1)	0.2332 (1)	O(32)	0.7926 (3)	−0.0364 (3)	0.3749 (6)
Ge(2)	0.6227 (1)	0.2173 (1)	0.2689 (1)	C(33)	0.8018 (3)	0.1165 (3)	0.0894 (5)
Fe(1)	1.0129 (1)	0.3155 (1)	0.2788 (1)	O(33)	0.7951 (3)	0.0991 (3)	−0.0339 (4)
Fe(2)	0.8852 (1)	0.3359 (1)	0.0165 (1)	C(41)	0.6399 (3)	0.4106 (3)	0.2440 (5)
Fe(3)	0.8134 (1)	0.1410 (1)	0.2867 (1)	O(41)	0.5948 (3)	0.4656 (3)	0.1571 (4)
Fe(4)	0.7099 (1)	0.3269 (1)	0.3842 (1)	C(42)	0.7782 (3)	0.3923 (3)	0.5064 (5)
Fe(5)	0.4807 (1)	0.2292 (1)	0.0887 (1)	O(42)	0.8170 (3)	0.4303 (3)	0.5936 (4)
Fe(6)	0.4983 (1)	0.1631 (1)	0.3667 (1)	C(43)	0.6085 (3)	0.3666 (3)	0.5050 (4)
C(11)	1.0888 (4)	0.1909 (4)	0.2033 (6)	O(43)	0.5443 (3)	0.4012 (3)	0.5844 (4)
O(11)	1.1412 (3)	0.1138 (3)	0.1624 (5)	Cb(1)	0.8010 (3)	0.2040 (3)	0.4897 (5)
C(12)	1.1118 (4)	0.3589 (4)	0.2352 (7)	Ob(1)	0.8319 (3)	0.1846 (3)	0.6081 (4)
O(12)	1.1729 (3)	0.3860 (3)	0.2109 (6)	C(51)	0.5627 (4)	0.1059 (3)	0.0178 (5)
C(13)	0.9357 (3)	0.4432 (3)	0.3429 (5)	O(51)	0.6112 (3)	0.0303 (3)	−0.0338 (4)
O(13)	0.8949 (3)	0.5215 (2)	0.3881 (4)	C(52)	0.4896 (4)	0.2752 (4)	−0.0765 (6)
C(14)	1.0443 (5)	0.2778 (4)	0.4617 (6)	O(52)	0.4917 (4)	0.3047 (3)	−0.1845 (5)
O(14)	1.0641 (4)	0.2547 (4)	0.5774 (5)	C(53)	0.3572 (4)	0.2108 (3)	0.0469 (5)
C(21)	0.9536 (4)	0.2068 (4)	−0.0496 (5)	O(53)	0.2804 (3)	0.1997 (3)	0.0163 (5)
O(21)	0.9945 (3)	0.1286 (3)	−0.1001 (5)	C(54)	0.4231 (3)	0.3573 (3)	0.1642 (5)
C(22)	0.9684 (5)	0.3758 (4)	−0.0780 (6)	O(54)	0.3857 (3)	0.4386 (3)	0.2037 (5)
O(22)	1.0186 (4)	0.4034 (4)	−0.1366 (5)	C(61)	0.5798 (4)	0.1377 (4)	0.5362 (5)
C(23)	0.8113 (4)	0.4643 (4)	0.0775 (5)	O(61)	0.6293 (4)	0.1210 (3)	0.6425 (4)
O(23)	0.7625 (3)	0.5457 (2)	0.1059 (4)	C(62)	0.3850 (4)	0.1348 (4)	0.3791 (6)
C(24)	0.7712 (4)	0.3340 (4)	−0.0962 (5)	O(62)	0.3132 (4)	0.1184 (4)	0.3939 (7)
O(24)	0.6983 (3)	0.3330 (4)	−0.1645 (5)	C(63)	0.5593 (4)	0.0359 (4)	0.2888 (5)
C(31)	0.9530 (3)	0.0821 (3)	0.3284 (5)	O(63)	0.5912 (3)	−0.0452 (3)	0.2481 (5)
O(31)	1.0382 (3)	0.0408 (3)	0.3608 (5)	C(64)	0.4183 (4)	0.2893 (4)	0.4341 (6)
C(32)	0.7956 (4)	0.0343 (3)	0.3402 (6)	O(64)	0.3629 (3)	0.3621 (3)	0.4813 (5)

Table III. Final Positional Parameters for $Sn_2Fe_6(CO)_{23}$ (**3a**)

atom	*x*	*y*	*z*	atom	*x*	*y*	*z*
Sn(1)	−0.1747 (2)	−0.0363 (2)	0.7563 (1)	O(32)	−0.435 (2)	0.179 (1)	0.725 (1)
Sn(2)	0.0141 (2)	0.2597 (2)	0.7935 (1)	C(33)	−0.164 (3)	0.245 (2)	0.932 (2)
Fe(1)	−0.3527 (5)	−0.2282 (3)	0.7350 (3)	O(33)	−0.162 (2)	0.318 (2)	0.983 (1)
Fe(2)	−0.2726 (5)	−0.1221 (3)	0.6005 (3)	C(41)	0.139 (3)	−0.048 (2)	0.868 (2)
Fe(3)	−0.1734 (5)	0.1352 (3)	0.8568 (3)	O(41)	0.186 (2)	−0.124 (2)	0.889 (1)
Fe(4)	0.1009 (5)	0.0819 (3)	0.8379 (3)	C(42)	0.145 (4)	0.069 (2)	0.737 (2)
Fe(5)	0.1728 (5)	0.4577 (3)	0.8361 (3)	O(42)	0.179 (2)	0.052 (1)	0.676 (1)
Fe(6)	−0.0221 (5)	0.3661 (3)	0.6674 (3)	C(43)	0.295 (3)	0.167 (2)	0.891 (2)
C(11)	−0.478 (3)	−0.346 (2)	0.665 (2)	O(43)	−0.104 (2)	0.511 (1)	0.885 (1)
O(11)	−0.556 (3)	−0.425 (2)	0.619 (2)	C(51)	0.230 (4)	0.593 (2)	0.810 (2)
C(12)	−0.360 (3)	−0.262 (2)	0.838 (2)	O(51)	0.275 (2)	0.676 (2)	0.797 (1)
O(12)	−0.368 (3)	−0.283 (2)	0.902 (2)	C(52)	0.263 (4)	0.461 (3)	0.935 (2)
C(13)	−0.510 (3)	−0.153 (2)	0.733 (2)	O(52)	0.334 (2)	0.479 (2)	1.013 (2)
O(13)	−0.604 (2)	−0.105 (2)	0.737 (1)	C(53)	0.003 (3)	0.490 (2)	0.866 (2)
C(14)	−0.180 (3)	−0.280 (2)	0.744 (2)	O(53)	0.422 (3)	0.214 (2)	0.927 (1)
O(14)	−0.070 (2)	0.681 (1)	0.757 (1)	C(54)	0.335 (4)	0.409 (2)	0.813 (2)
C(21)	−0.388 (4)	−0.237 (2)	0.522 (2)	O(54)	0.443 (2)	0.380 (2)	0.795 (1)
O(21)	−0.459 (3)	−0.311 (2)	0.471 (2)	C(61)	0.029 (4)	0.489 (3)	0.628 (2)
C(22)	−0.188 (3)	−0.019 (2)	0.546 (2)	O(61)	0.074 (3)	0.572 (2)	0.600 (2)
O(22)	−0.122 (2)	0.047 (1)	0.518 (1)	C(62)	−0.157 (4)	0.284 (3)	0.578 (2)
C(23)	−0.437 (4)	−0.058 (2)	0.596 (2)	O(62)	−0.250 (3)	0.242 (2)	0.512 (2)
O(23)	−0.541 (2)	−0.011 (2)	0.590 (1)	C(63)	−0.189 (3)	0.406 (2)	0.696 (2)
C(24)	−0.093 (3)	−0.174 (2)	0.615 (2)	O(63)	−0.298 (2)	0.433 (2)	0.709 (1)
O(24)	0.025 (2)	−0.199 (1)	0.623 (1)	C(64)	0.132 (3)	0.306 (2)	0.640 (2)
C(31)	−0.290 (3)	0.046 (2)	0.901 (2)	O(64)	0.223 (3)	0.268 (2)	0.620 (1)
O(31)	−0.380 (2)	−0.015 (2)	0.931 (1)	C(1)	0.031 (3)	0.113 (2)	0.938 (2)
C(32)	−0.332 (4)	0.163 (2)	0.773 (2)	O(1)	0.069 (2)	0.118 (1)	1.012 (1)

$Fe_2(CO)_9$ with Ge_2H_6 at 68 °C for 15–20 min, the yields of **3b** and particularly **4b** are much enhanced at the expense of $Ge[Fe_2(CO)_8]_2$, allowing sufficient material to be isolated for crystallographic characterization. The green **2b** was not seen. The overall recovery of products was similar for both hydrides at around 60%, reflecting high conversions of Ge when handling losses are taken into account. For both hydrides, all the hydrogen appears as H_2, but the formation of CO is variable and low, suggesting that much of this ends up as $Fe(CO)_5$, which was clearly identified but not separated quantitatively from the solvent. The reaction may be summarized by the general equation (1).

$$GeH_4 + Fe_2(CO)_9 \rightarrow H_2 + CO + Fe(CO)_5 + Fe_3(CO)_{12} + \underset{\mathbf{1b}}{Ge[Fe_2(CO)_8]_2} + \underset{\mathbf{3b}}{Ge_2Fe_6(CO)_{23}} + \underset{\mathbf{4b}}{Ge_2Fe_7(CO)_{26}} + \underset{\mathbf{2b}}{GeFe_5(CO)_{19}} \quad (1)$$

A similar equation applies for the reaction with Ge_2H_6, only the relative amounts of the different clusters being altered. In the higher conversion of Ge_2H_6 to digermanium products, these $Fe_2(CO)_9$ reactions resemble those[14] of $Co_2(CO)_8$, where $GeCo_4(CO)_{14}$, the analogue of **1b**, is the major product from GeH_4 and $Ge_2Co_6(CO)_{20}$, likewise related to **3b**, is the major product from Ge_2H_6.

In the related reaction of SnH_4 with $Fe_2(CO)_9$ rapid workup allowed the separation of orange **3a** and a red-brown species that has spectroscopic properties compatible with its being the $Sn_2Fe_7(CO)_{26}$ cluster **4a**, the tin analogue of **4b**. Both the tin and germanium systems have parallels in the range of clusters formed, but the relative yields differ for the two systems. Thus, **2a** is the major higher cluster from the tin system whereas **2b** was a very minor component under all conditions tried in the germanium reactions.

Table IV. Final Positional Parameters for $Ge_2Fe_7(CO)_{26}$ (**4b**)

atom	*x*	*y*	*z*
Ge(1)	0.8629 (3)	0.1391 (3)	0.7254 (2)
Ge(2)	0.8701 (3)	0.1835 (3)	0.9068 (2)
Fe(1)	0.9564 (3)	0.1340 (3)	0.6583 (2)
Fe(2)	0.8234 (4)	0.0411 (4)	0.6649 (3)
Fe(3)	0.7910 (4)	0.2506 (3)	0.7564 (3)
Fe(4)	0.8745 (4)	0.1481 (3)	0.8171 (2)
Fe(5)	0.7918 (4)	0.2734 (3)	0.8576 (2)
Fe(6)	0.8393 (4)	0.1125 (3)	0.9841 (2)
Fe(7)	0.9691 (4)	0.2120 (4)	0.9683 (2)
C(1)	0.743 (3)	0.327 (3)	0.801 (2)
O(1)	0.698 (1)	0.385 (1)	0.794 (1)
C(11)	1.013 (3)	0.068 (3)	0.695 (2)
O(11)	1.049 (2)	0.027 (2)	0.720 (1)
C(12)	1.020 (2)	0.210 (2)	0.674 (2)
O(12)	1.061 (2)	0.261 (2)	0.687 (1)
C(13)	0.998 (3)	0.096 (3)	0.599 (2)
O(13)	1.017 (2)	0.068 (2)	0.561 (1)
C(14)	0.900 (3)	0.202 (3)	0.627 (2)
O(14)	0.862 (1)	0.246 (2)	0.604 (1)
C(21)	0.881 (3)	−0.030 (2)	0.700 (2)
O(21)	0.920 (2)	−0.079 (2)	0.714 (1)
C(22)	0.750 (3)	0.006 (3)	0.693 (2)
O(22)	0.691 (2)	−0.026 (2)	0.713 (1)
C(23)	0.833 (3)	−0.007 (3)	0.605 (2)
O(23)	0.843 (2)	−0.034 (2)	0.566 (1)
C(24)	0.765 (2)	0.113 (2)	0.639 (2)
O(24)	0.714 (2)	0.153 (2)	0.620 (1)
C(31)	0.878 (2)	0.309 (2)	0.749 (2)
O(31)	0.929 (2)	0.346 (2)	0.737 (1)
C(32)	0.705 (2)	0.185 (2)	0.758 (2)
O(32)	0.657 (2)	0.146 (2)	0.751 (1)
C(33)	0.752 (3)	0.292 (3)	0.700 (2)
O(33)	0.727 (1)	0.323 (2)	0.665 (1)
C(41)	0.959 (2)	0.203 (2)	0.812 (2)
O(41)	1.020 (2)	0.234 (2)	0.810 (1)
C(42)	0.788 (3)	0.085 (3)	0.826 (2)
O(42)	0.741 (2)	0.038 (2)	0.830 (1)
C(43)	0.930 (3)	0.065 (3)	0.821 (2)
O(43)	0.969 (2)	0.011 (2)	0.827 (1)
C(51)	0.881 (2)	0.330 (2)	0.856 (2)
O(51)	0.926 (2)	0.379 (2)	0.862 (1)
C(52)	0.715 (3)	0.208 (2)	0.876 (2)
O(52)	0.665 (2)	0.169 (2)	0.885 (1)
C(53)	0.751 (2)	0.331 (2)	0.903 (2)
O(53)	0.719 (2)	0.373 (2)	0.932 (1)
C(61)	0.898 (3)	0.035 (3)	0.961 (2)
O(61)	0.940 (2)	−0.018 (2)	0.949 (1)
C(62)	0.759 (2)	0.057 (2)	0.966 (2)
O(62)	0.704 (2)	0.026 (2)	0.950 (1)
C(63)	0.776 (2)	0.192 (2)	1.002 (2)
O(63)	0.732 (2)	0.242 (2)	1.010 (1)
C(64)	0.862 (3)	0.091 (3)	1.053 (2)
O(64)	0.867 (2)	0.072 (2)	1.092 (2)
C(71)	0.906 (3)	0.300 (4)	0.988 (2)
O(71)	0.872 (2)	0.351 (2)	0.998 (1)
C(72)	1.032 (2)	0.273 (2)	0.941 (1)
O(72)	1.077 (2)	0.318 (2)	0.918 (1)
C(73)	1.019 (3)	0.139 (3)	0.939 (2)
O(73)	1.059 (2)	0.092 (2)	0.919 (1)
C(74)	1.011 (2)	0.199 (2)	1.031 (2)
O(74)	1.034 (2)	0.190 (2)	1.071 (1)

Table V. Selected Bond Lengths and Angles for $Ge_2Fe_6(CO)_{23}$ (**3b**)

Bond Lengths (Å)			
Ge(1)–Fe(1)	2.408 (1)	Ge(2)–Fe(5)	2.380 (1)
Ge(1)–Fe(2)	2.379 (1)	Ge(2)–Fe(6)	2.452 (1)
Ge(1)–Fe(3)	2.438 (1)	Fe(1)–Fe(2)	2.789 (1)
Ge(1)–Fe(4)	2.423 (1)	Fe(3)–Fe(4)	2.634 (1)
Ge(2)–Fe(3)	2.436 (1)	Fe(3)–Cb(1)	1.980 (4)
Ge(2)–Fe(4)	2.428 (1)	Fe(4)–Cb(1)	2.028 (4)
		Fe(5)–Fe(6)	2.794 (1)
Bond Angles (deg)			
Fe(1)–Ge(1)–Fe(2)	71.3 (1)	Fe(5)–Ge(2)–Fe(6)	70.7 (1)
Fe(1)–Ge(1)–Fe(3)	132.1 (1)	Ge(1)–Fe(1)–Fe(2)	53.9 (1)
Fe(1)–Ge(1)–Fe(4)	129.4 (1)	Ge(1)–Fe(2)–Fe(1)	54.8 (1)
Fe(2)–Ge(1)–Fe(3)	134.5 (1)	Ge(1)–Fe(3)–Ge(2)	100.2 (1)
Fe(2)–Ge(1)–Fe(4)	136.1 (1)	Ge(1)–Fe(3)–Fe(4)	56.9 (1)
Fe(3)–Ge(1)–Fe(4)	65.6 (1)	Ge(2)–Fe(3)–Fe(4)	57.1 (1)
Fe(3)–Ge(2)–Fe(4)	65.6 (1)	Ge(1)–Fe(4)–Ge(2)	100.8 (1)
Fe(3)–Ge(2)–Fe(5)	137.8 (1)	Ge(1)–Fe(4)–Fe(3)	57.5 (1)
Fe(3)–Ge(2)–Fe(6)	128.7 (1)	Ge(2)–Fe(4)–Fe(3)	57.4 (1)
Fe(4)–Ge(2)–Fe(5)	136.5 (1)	Ge(2)–Fe(5)–Fe(6)	55.9 (1)
Fe(4)–Ge(2)–Fe(6)	129.5 (1)	Ge(2)–Fe(6)–Fe(5)	53.5 (1)
Dihedral Angles (deg)			
Ge(1)Fe(1)Fe(2)/Ge(1)Fe(3)Fe(4)	87.5		
Ge(2)Fe(3)Fe(4)/Ge(2)Fe(5)Fe(6)	88.8		
Ge(1)Fe(3)Fe(4)/Ge(2)Fe(3)Fe(4)	132.3		

Table VI. Selected Bond Lengths and Angles for $Sn_2Fe_6(CO)_{23}$ (**3a**)

Bond Lengths (Å)			
Sn(1)–Fe(1)	2.555 (4)	Sn(2)–Fe(4)	2.612 (4)
Sn(1)–Fe(2)	2.529 (5)	Sn(2)–Fe(5)	2.543 (5)
Sn(1)–Fe(3)	2.564 (4)	Sn(2)–Fe(6)	2.563 (5)
Sn(1)–Fe(4)	2.570 (4)	Fe(1)–Fe(2)	2.857 (6)
Sn(2)–Fe(3)	2.552 (4)	Fe(3)–Fe(4)	2.734 (5)
		Fe(5)–Fe(6)	2.862 (7)
Bond Angles (deg)			
Fe(1)–Sn(1)–Fe(2)	68.4 (1)	Fe(5)–Sn(2)–Fe(6)	68.2 (2)
Fe(1)–Sn(1)–Fe(3)	127.4 (2)	Sn(1)–Fe(1)–Fe(2)	55.4 (1)
Fe(1)–Sn(1)–Fe(4)	142.9 (2)	Sn(1)–Fe(2)–Fe(1)	56.2 (1)
Fe(2)–Sn(1)–Fe(3)	141.0 (2)	Sn(1)–Fe(3)–Sn(2)	92.4 (1)
Fe(2)–Sn(1)–Fe(4)	128.2 (2)	Sn(1)–Fe(3)–Fe(4)	57.9 (1)
Fe(3)–Sn(1)–Fe(4)	64.4 (1)	Sn(2)–Fe(3)–Fe(4)	59.1 (1)
Fe(3)–Sn(2)–Fe(4)	63.9 (1)	Sn(1)–Fe(4)–Sn(2)	90.9 (1)
Fe(3)–Sn(2)–Fe(5)	134.4 (2)	Sn(1)–Fe(4)–Fe(3)	57.7 (1)
Fe(3)–Sn(2)–Fe(6)	134.8 (2)	Sn(2)–Fe(4)–Fe(3)	57.0 (1)
Fe(4)–Sn(2)–Fe(5)	128.2 (2)	Sn(2)–Fe(5)–Fe(6)	56.2 (1)
Fe(4)–Sn(2)–Fe(6)	140.9 (2)	Sn(2)–Fe(6)–Fe(5)	55.6 (1)
Dihedral Angles (deg)			
Sn(1)Fe(1)Fe(2)/Sn(1)Fe(3)Fe(4)	73.1		
Sn(2)Fe(3)Fe(4)/Sn(2)Fe(5)Fe(6)	82.7		
Sn(1)Fe(3)Fe(4)/Sn(2)Fe(3)Fe(4)	115.8		

These reactions contrast markedly with the reaction of SiH_4 with $Fe_2(CO)_9$ where only **1d** formed, with little evidence for higher clusters.[7] This observation was reinforced by the disilane study, which also showed no sign of stable Si analogues of **2**, **3**, or **4**. A major product was a soluble, fairly unstable, red species whose IR spectrum and behavior indicated it was the same as that found as a minor product in the SiH_4 reactions[7] and probably similar to the red product from GeH_4 reacting at lower temperatures. From the H_2 figure, only about one-third of the reacted disilane forms **1d** and the rest may form this red compound. We note the formation of $Fe_3(CO)_{12}$, which must be a secondary reaction product, possibly from the red species, as it increases on handling and would not form directly from $Fe_2(CO)_9$ under the reaction conditions.

Structural Studies. To fully define the new clusters, the structures of **3a**, **3b**, and **4b** were examined by X-ray crystallography. The clusters $Ge_2Fe_6(CO)_{23}$ (**3b**) and $Sn_2Fe_6(CO)_{23}$ (**3a**) both form triclinic crystals but are not isomorphous, although they are essentially isostructural, differing only in small details (Figures 1 and 2). They consist of four linked EFe_2 (E = Ge, Sn) triangles and may be described in several ways. They are the first homologues of **1b** or **1a**, requiring the bridging carbonyl to provide an 18-electron count at each of the central atoms. Alternatively they can be regarded as derivatives of $Fe_2(CO)_9$, where two of the bridging carbonyls have been replaced by μ-E[$Fe_2(CO)_8$] units. An exactly analogous structure is found[15,16] in $Ge_2Co_4Fe_2(CO)_{21}$

---

(16) Anema, S. G.; Audett, J. A.; Mackay, K. M.; Nicholson, B. K. *J. Chem. Soc., Dalton Trans.* **1988**, 2629.

(17) Raubenheimer, H. G.; Kruger, G. J.; Lombard, A. V. A. *J. Organomet. Chem.* **1987**, *323*, 385.

Table VII. Selected Bond Lengths and Angles for $Ge_2Fe_7(CO)_{26}$ (**4b**)

Bond Angles (Å)			
Ge(1)-Fe(1)	2.373 (8)	Ge(2)-Fe(6)	2.402 (8)
Ge(1)-Fe(2)	2.395 (8)	Ge(2)-Fe(7)	2.385 (8)
Ge(1)-Fe(3)	2.415 (8)	Fe(1)-Fe(2)	2.798 (8)
Ge(1)-Fe(4)	2.387 (8)	Fe(3)-Fe(4)	2.763 (9)
Ge(2)-Fe(4)	2.402 (8)	Fe(3)-Fe(5)	2.650 (9)
Ge(2)-Fe(5)	2.413 (7)	Fe(4)-Fe(5)	2.784 (8)
		Fe(6)-Fe(7)	2.845 (9)
Bond Angles (deg)			
Fe(1)-Ge(1)-Fe(2)	71.9 (2)	Ge(1)-Fe(3)-Fe(4)	54.4 (2)
Fe(1)-Ge(1)-Fe(3)	128.5 (3)	Ge(1)-Fe(3)-Fe(5)	116.3 (3)
Fe(1)-Ge(1)-Fe(4)	132.3 (3)	Fe(4)-Fe(3)-Fe(5)	61.9 (2)
Fe(2)-Ge(1)-Fe(3)	128.8 (3)	Ge(1)-Fe(4)-Ge(2)	167.2 (3)
Fe(2)-Ge(1)-Fe(4)	135.9 (3)	Ge(1)-Fe(4)-Fe(3)	55.4 (2)
Fe(3)-Ge(1)-Fe(4)	70.2 (3)	Ge(1)-Fe(4)-Fe(5)	112.4 (3)
Fe(4)-Ge(2)-Fe(5)	70.7 (2)	Ge(2)-Fe(4)-Fe(3)	111.9 (3)
Fe(4)-Ge(2)-Fe(6)	133.2 (3)	Ge(2)-Fe(4)-Fe(5)	54.9 (2)
Fe(4)-Ge(2)-Fe(7)	132.4 (3)	Fe(3)-Fe(4)-Fe(5)	57.1 (2)
Fe(5)-Ge(2)-Fe(6)	129.8 (3)	Ge(2)-Fe(5)-Fe(3)	115.5 (3)
Fe(5)-Ge(2)-Fe(7)	128.4 (3)	Ge(2)-Fe(5)-Fe(4)	54.5 (2)
Fe(6)-Ge(2)-Fe(7)	72.9 (2)	Fe(3)-Fe(5)-Fe(4)	61.0 (2)
Ge(1)-Fe(1)-Fe(2)	54.4 (2)	Ge(2)-Fe(6)-Fe(7)	53.3 (2)
Ge(1)-Fe(2)-Fe(1)	53.7 (2)	Ge(2)-Fe(7)-Fe(6)	53.8 (2)
		Fe(3)-C(1)-Fe(5)	86 (2)
Dihedral Angles (deg)			
Ge(1)Ge(2)Fe(3)Fe(4)Fe(5)/Ge(1)Fe(1)Fe(2)	87.5		
Ge(1)Ge(2)Fe(3)Fe(4)Fe(5)/Ge(2)Fe(6)Fe(7)	89.3		

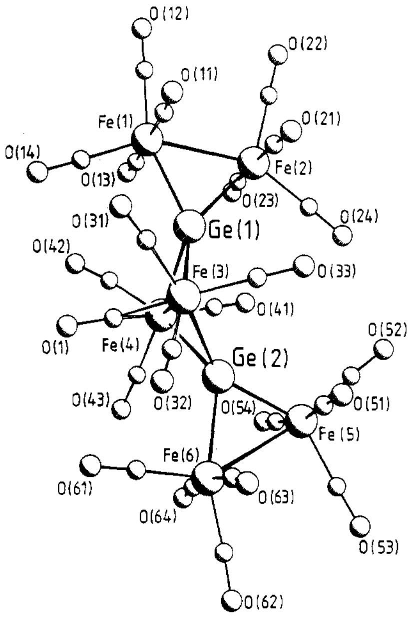

Figure 1. PLUTO diagram of the structure of $Ge_2Fe_6(CO)_{23}$ (**3b**).

(**5**), where the bridging units are μ-Ge[$Co_2(CO)_7$], while a similar structure has been proposed[14] for $Ge_2Co_6(CO)_{20}$ (**6**).

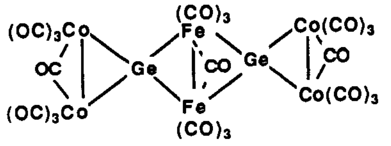

5

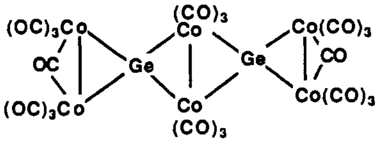

6

For **3b** the central Fe–Fe bond is 2.634 (1) Å, longer than that of $Fe_2(CO)_9$ at 2.523 (1) Å,[18] as a consequence of replacing two of the bridging carbonyl groups by Ge atoms. The external Fe–Fe bonds are even longer at 2.791 (1) Å, consistent with there being only one, large bridging atom. The Ge–Fe distances fall into two groups; those to the central iron atoms average 2.431 (1) Å, while those to the peripheral iron atoms average 2.405 (1) Å. The dihedral angles between the triangles with a common Ge apex are 87.5 (1)° at Ge(1) and 88.8 (1)° at Ge(2), which are close to the expected perpendicular arrangement. However, the dihedral angle between the triangles sharing a common Fe(3)–Fe(4) edge is very wide at 132.3 (1)°, suggesting there are considerable steric interactions between the opposite ends of the molecule. The Ge···Ge nonbonded distance is 3.74 Å. For the related mixed-metal cluster $Ge_2Fe_2Co_4(CO)_{21}$ (**5**) the corresponding dihedral angle was only 111°, with a Ge···Ge distance of 3.30 Å, suggesting that it is the packing of the different numbers of CO groups that directs the core geometry.

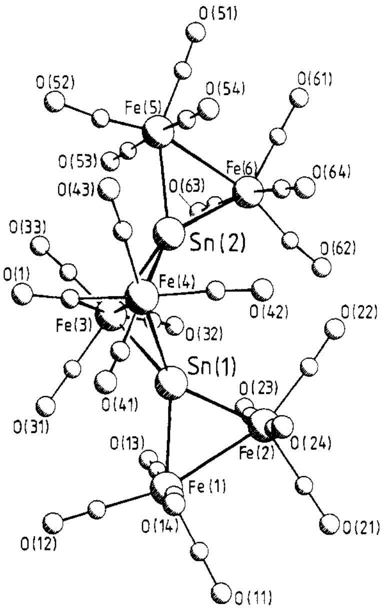

Figure 2. PLUTO diagram of the structure of $Sn_2Fe_6(CO)_{23}$ (**3a**).

For **3a** the Sn–Fe and Fe–Fe bonds are as expected by comparison with **3b**, allowing for the larger size of Sn compared to Ge. Thus, the inner Sn–Fe bonds (2.575 (4) Å average) and outer Sn–Fe bonds (2.547 (4) Å average) are both about 0.14 Å longer than the Ge–Fe bonds in the germanium analogue. The outer Fe–Fe bond has expanded by 0.05 Å and the inner by 0.10 Å on going from **3b** to **3a**, reflecting the change of one and two bridging groups, respectively, from Ge to Sn. These variations are in accord with those of simpler species such as **1**.

The germanium and tin compounds **3** add to the slowly growing list of 102-electron, linked-triangle clusters with similar E_2M_6 cores and *spiro*-E atoms. In addition to **5**, and the postulated structure **6**, this group includes $Sb_2Fe_6(CO)_{22}$[11] and $S_2Fe_6(CO)_{18}(\mu\text{-}CNEt_2)_2$.[17] An interesting comparison is between **3a** and $Sb_2Fe_6(CO)_{22}$, which has five-electron Sb in place of four-electron Sn and one fewer CO to maintain the same electron count.[11] The inner Fe–Fe bond is 0.113 Å shorter in the Sn example, no doubt because of the μ-CO group, while the outer Fe–Fe bonds are similar. The most noticeable feature is that for $Sb_2Fe_6(CO)_{22}$ the inner Sb–Fe bonds are *shorter* than the outer ones, in direct contrast to the distribution of the Sn–Fe bonds of **3a**, since the Sb atoms act as three-electron donors toward the central Fe_2 group and as two-electron donors to the outer ones.[11]

The dihedral angles between $SnFe_2$ triangles in **3a** are markedly different from those of **3b**. The two triangles with a common apex at Sn(1) have a dihedral angle of 73.1 (1)°, while for those at Sn(2) the equivalent value is 83°, the former especially being well removed from the expected perpendicular value. On the other hand, the butterfly angle between the two central triangles is 115.8

---

(18) Cotton, F. A.; Troup, J. M. *J. Chem. Soc., Dalton Trans.* **1974**, 800.

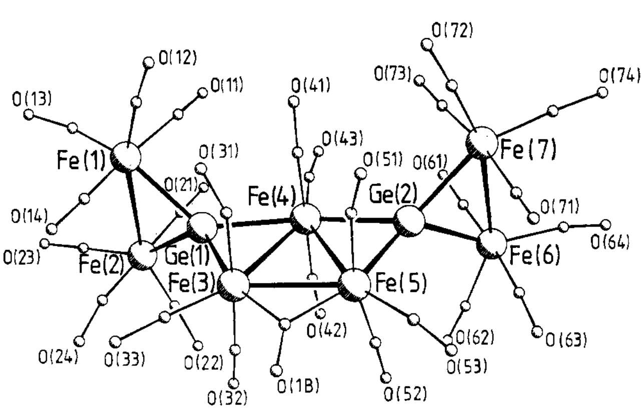

Figure 3. Perspective view of the structure of $Ge_2Fe_7(CO)_{26}$ (**4b**).

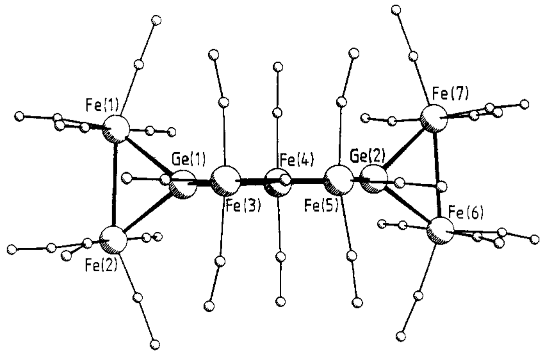

Figure 4. $Ge_2Fe_7(CO)_{26}$ (**4b**) viewed along the bridging carbonyl vector, showing the planarity of the central core and the near-orthogonality of the triangles outer to the core.

(1)°, closer to the expected 120° than the corresponding value in the germanium cluster; the Sn···Sn distance is 3.69 Å. It appears that in **3a** the steric interactions are relieved by twisting about the *spiro*-tin atoms, while in **3b** an opening about the central Fe–Fe "hinge" is preferred. From the relatively large variations found for these and the other E_2Fe_6 clusters,[11,17] it can be concluded that the metal core is quite flexible. The ease of deformation of the framework is also apparent in the varying small degrees of asymmetry in the EFe_2 triangles making up the clusters discussed here.

The structure of $Ge_2Fe_7(CO)_{26}$ (**4b**) is shown in Figure 3. It is based on a triangle of Fe atoms bridged along all three edges, in a manner similar to that found in $[(CO)_3RuGeMe_2]_3$.[19] There are μ-$Ge[Fe_2(CO)_8]$ units bridging two of the edges of the central Fe_3 triangle, while the third edge is bridged by a nearly symmetrically placed CO. As Figure 4 shows, the central Ge_2Fe_5 skeleton is essentially planar, with the outer $GeFe_2$ triangles virtually perpendicular to this plane. None of the eight Ge–Fe bonds differ significantly from the mean value of 2.40 Å, which is the same as that found for $Ge[Fe_2(CO)_8]_2$ (**1b**). The outer Fe–Fe bonds are the same as the equivalent bonds in **1b**, while the inner Fe–Fe bonds bridged by Ge appear marginally shorter, with the CO-bridged bond the shortest of all. However, a detailed comparison of parameters is precluded by the poor quality of the data available (see Experimental Section). The central core of complex **4b** also relates to "raft" clusters such as $Os_6(CO)_{21}$, which are currently of particular interest.[20]

The crystal structures of **4b** and **2a**[9] establish two different types based on the Fe_3 triangle, and the spectroscopic evidence for the analogue **4a** is reasonable. The Ge analogue of **2a** may also have been formed, but the evidence is slight. **2a** relates simply to the structure of $Fe_3(CO)_{12}$, by replacing one μ-CO group with a μ-$Sn[Fe_2(CO)_8]$ unit along one of the Fe–Fe edges,[9] and the compound retains the distinctive green color of most simple $Fe_3(CO)_{12}$ derivatives. Replacing two carbonyls with μ-$Ge[Fe_2(CO)_8]$ groups gives a marked color change and a different structure, **4b**, presumably a steric requirement since two bulky groups are unlikely to bridge a single edge of an Fe_3 triangle. We note $M_3(CO)_{10}[\mu\text{-}SnR_2]_2$ [M = Ru, Os; R = $CH(SiMe_3)_2$] adopts the same basic arrangement as **4b**,[21] while $Ru_3(CO)_9(\mu\text{-}GeMe_2)_3$ relates by replacing the last bridging carbonyl.[19] It may be that a corresponding $Fe_3(CO)_9[\mu\text{-}E\{Fe_2(CO)_8\}]_3$ (E = Ge, Sn) is among the minor unidentified products that are formed in the reactions described herein; this would be a splendid example of a D_{3h} molecule (compare Figure 3).

The structural feature common to all these products of hydride reactions with $Fe_2(CO)_9$ is the $EFe_2(CO)_8$ triangle with an Fe–Fe bond unbridged by CO. The isomeric $PbFe_2(CO)_6(\mu\text{-}CO)_2$ form was crystallographically established[22] in $[Pb\{Fe_2(CO)_8\}\{Fe(CO)_4\}_2]^{2-}$, with the Sn analogue[6] probably the same. However, the nonbridged form is more widely established, not only in the molecules here but also in a crystal structure[23] of the pentaphenylgermole $Ph_5C_4GeFe_2(CO)_8$ and, on spectroscopic grounds, in $R_2EFe_2(CO)_8$ for R_2E = Me_2Si,[24] Ph_2Ge,[25] and $[(Me_3Si)_2CH]_2Sn$.[26]

The reaction[6] of GeI_2 with $[Fe_2(CO)_8]^{2-}$ produces $[GeFe_4(CO)_{14}]^{2-}$, whose structure is similar to that of the isoelectronic $GeCo_4(CO)_{13}$[27] with a GeM_3 trigonal pyramid carrying an apical $(CO)_4M$ unit bonded to the Ge. In contrast, closo species have not been found in these germane reactions. Nor has there been any indication of four-membered E_2Fe_2 rings, such as was found[16] en route to **5** and in compounds such as $Sn[Fe_2(CO)_8(\mu\text{-}SnMe_2)]_2$.[24] Clearly, we are seeing only the beginning of a very rich field.

Vibrational Spectra of 3b. Relatively few Raman spectra of linked-triangle clusters have been reported, and it was pleasing that **3b** resisted photodegradation. The carbonyl region showed intensities largely complementary to the infrared bands, and the bridging mode was too weak to detect.

The other region of interest is that below 300 cm^{-1}, and the Raman shifts for **3b** at 288, 232, 202, and 182 cm^{-1} and the IR bands at 278 and 246 cm^{-1} are assigned as stretching modes of the heavy-atom skeletons, while the lower frequency modes for both species involve more bending contribution. These frequencies compare with ν(Ge–Fe) bands at 229 and 216 cm^{-1} in $(GeH_3)_2Fe(CO)_4$ and similar species.[28] Preliminary results for **1d** gave a strong polarized band at 196 cm^{-1}, assigned as the in-phase stretch of the $SiFe_4$ skeleton. Similar cobalt compounds with linked $GeCo_2$ triangle skeletons also show heavy-atom modes over the range 180–280 cm^{-1}.

Reaction Path. We suggest that all the products of these reactions of group 14 hydrides with $Fe_2(CO)_9$ may be simply rationalized by two basic steps—the formation of an $EFe_2(CO)_8$ triangle and the addition of an $Fe(CO)_x$ unit. Initially, a hydride reacts with $Fe_2(CO)_9$ to replace one μ-CO by μ-EH_2 and the two remaining μ-CO's rearrange into the isomeric $H_2E\{Fe(CO)_4\}_2$ form. Repeating this step yields the molecules **1**, while attack of two such species on the same $Fe_2(CO)_9$ molecule yields **3**. All the displaced H is recovered as H_2, while only a small proportion of the CO is found, and it is thought that most reacts with iron

---

(19) Howard, J. A. K.; Knox, S. A. R.; Stone, F. G. A.; Woodward, P. *J. Chem. Soc. D* **1970**, 1477. Howard, J. A. K.; Woodward, P. *J. Chem. Soc. A* **1971**, 3648.

(20) Goudsmit, R. J.; Jeffrey, J. G.; Johnson, B. F. G.; Lewis, J.; McQueen, R. S. C.; Sanders, A. J.; Liu, J.-C. *J. Chem. Soc., Chem. Commun.* **1986**, 24. Mingos, D. M. P.; Evans, D. G. *Organometallics* **1983**, *2*, 35.

(21) Cardin, C. J.; Cardin, D. J.; Lawless, G. A.; Power, J. M.; Power, M. B. *J. Organomet. Chem.* **1987**, *325*, 203.

(22) Lagrone, C. B.; Whitmire, K. H.; Churchill, M. R.; Fettinger, J. C. *Inorg. Chem.* **1986**, *25*, 2080.

(23) Curtis, M. D.; Butler, W. M.; Scibelli, J. *J. Organomet. Chem.* **1980**, *192*, 209.

(24) Bikovetz, A. L.; Kuzmin, O. V.; Vdovin, V. M.; Krapivin, A. M. *J. Organomet. Chem.* **1980**, *194*, C33.

(25) Bonny, A. *Coord. Chem. Rev.* **1978**, *25*, 229.

(26) Cotton, J. D.; Davidson, P. J.; Lappert, M. F.; Donaldson, J. D.; Silver, J. *J. Chem. Soc., Dalton Trans.* **1976**, 2286.

(27) Schmid, G.; Etzrodt, G. *J. Organomet. Chem.* **1977**, *137*, 367.

(28) Audett, J. A.; Mackay, K. M. *J. Chem. Soc., Dalton Trans.* **1988**, 2635. Stobart, S. R. *J. Chem. Soc., Dalton Trans.* **1978**, 2442.

3164 Inorg. Chem. 1989, 28, 3164-3170

carbonyl species to give the observed $Fe(CO)_5$. This process may then be the source of an $Fe(CO)_x$ fragment that adds across the Fe–Fe bond of **1** to form **2**, or of **3** to form **4**, and also possibly reacts with $Fe_2(CO)_9$ to form part of the $Fe_3(CO)_{12}$ group. However, the various systems yielded increasing amounts of $Fe_3(CO)_{12}$ on workup, so that the characterized species such as **3** and **4** and, especially, the uncharacterized red species are probably its prime source. Under the reaction conditions of these experiments, $Fe_3(CO)_{12}$ does not form **2** or **4** in direct reaction with the hydrides, and $Fe(CO)_5$ does not react at all. Ge_2H_6 gives enhanced yields of **3b** and **4b** compared with those from GeH_4, showing that the two Ge atoms tend to occur together in the intermediates.

The Sn–Fe system is somewhat richer than the Ge–Fe one, while the Si–Fe one is much more limited. This suggests that Sn is the best match in size to form the critical EFe_2 unit. These comments are only a preliminary rationalization of the observed structures. The reaction systems reported in this and earlier[7,9] papers are complex ones, which are not always fully reproducible and are not yet completely understood. Other species are undoubtedly present and perhaps accessible by modified preparations. Of particular interest would be the replacement of the third μ-CO in **4** and the species related to **3** by the presence of a central four-membered ring, as found for **5**.

Acknowledgment. We thank Dr. Ward T. Robinson, University of Canterbury, for collection of X-ray intensity data. Acknowledgment is made to the New Zealand Universities Grants Committee and to the donors of the Petroleum Research Fund, administered by the American Chemical Society, for financial support.

Supplementary Material Available: Tables giving full crystallographic details, thermal parameters, all bond lengths and angles, and equations of least-squares planes (14 pages); tables of calculated and observed structure factors (50 pages). Ordering information is given on any current masthead page.

Contribution from the Department of Chemistry,
Rice University, Houston, Texas 77251

Synthesis, Characterization, and Reactivity of Iron Carbonyl Clusters Containing Bismuth or Antimony. Crystal Structures of Isomorphous $[Et_4N][BiFe_3Cr(CO)_{17}]$ and $[Et_4N][SbFe_3Cr(CO)_{17}]$ and the Ring Complex $Bi_2Fe_2(CO)_8Me_2$

Kenton H. Whitmire,* Minghuey Shieh, and Juanita Cassidy

Received September 29, 1988

The reaction of $[Et_4N]_2[Fe_2(CO)_8]$ with $BiCl_3$ or $SbCl_3$ forms compounds (Ia, E = Bi; Ib, E = Sb) that are proposed to be the previously characterized $[Et_4N][EClFe_3(CO)_{12}]$ based on elemental analyses and spectroscopic data. Treatment of Ia or Ib with $Cr(CO)_5(THF)$ produces $[Et_4N][EFe_3Cr(CO)_{17}]$ (IIa and IIb, respectively), while the methylation of Ia affords $Bi_2Fe_2(CO)_8Me_2$ (III). Refluxing Ia and Ib in acetonitrile gives the previously known $[Et_4N]_2[Bi_2Fe_4(CO)_{13}]$ and $[Et_4N]_2[Sb_2Fe_5(CO)_{17}]$, respectively. IIa, IIb, and III have been characterized by X-ray crystallography. IIa crystallizes in the centrosymmetric triclinic space group $P\bar{1}$ (no. 2) with $a = 12.297$ (3) Å, $b = 15.154$ (3) Å, $c = 9.791$ (1) Å, $\alpha = 107.60$ (1)°, $\beta = 95.24$ (2)°, $\gamma = 92.02$ (2)°, $V = 1727.9$ (6) $Å^3$, and $Z = 2$. The structure was refined to $R = 4.5\%$ and $R_w = 5.3\%$ for those 5114 reflections with $I > 3\sigma(I)$. The core framework of IIa consists of a distorted tetrahedral $BiFe_3Cr$ cluster in which a central bismuth atom is bonded to isolated $Fe(CO)_4$ and $Cr(CO)_5$ groups and a metal–metal-bonded $Fe_2(CO)_8$ fragment. The Fe–Fe bond distance is 2.608 (2) Å, and the Fe1–Bi1–Fe2 angle is 56.91 (4)°. IIb is isomorphous with IIa: centrosymmetric triclinic space group $P\bar{1}$ (no. 2), $a = 12.233$ (1) Å, $b = 15.108$ (5) Å, $c = 9.742$ (3) Å, $\alpha = 107.23$ (3)°, $\beta = 94.61$ (2)°, $\gamma = 92.37$ (1)°, $V = 1710.0$ (9) $Å^3$, and $Z = 2$. Diffraction data were refined to $R = 4.2\%$ and $R_w = 5.7\%$ for those 6100 reflections with $I > 3\sigma(I)$. The Fe–Fe bond distance in IIb is 2.598 (1) Å. III crystallizes in the centrosymmetric triclinic space group $P\bar{1}$ (no. 2) with $a = 7.571$ (4) Å, $b = 8.734$ (4) Å, $c = 7.136$ (3) Å, $\alpha = 107.02$ (4)°, $\beta = 108.41$ (4)°, $\gamma = 79.89$ (4)°, $V = 426.3$ (4) $Å^3$, and $Z = 1$. Refinement converged at $R = 4.1\%$ and $R_w = 5.3\%$ for those 1355 reflections with $I > 3\sigma(I)$. III consists of a Bi_2Fe_2 parallelogram situated about a crystallographic inversion center. There is one Me group bonded to each bismuth atom. The $Fe(CO)_4$ groups are pseudooctahedral with an average Bi–Fe distance of 2.786 Å. The Bi–C distance is 2.28 (1) Å.

Introduction

In recent years, heavy main-group atoms bonded to transition-metal fragments have been shown to adopt unexpected structures that range from electron-deficient planar molecules[1,2] to electron-rich environments as found in $[Cp_2Co][Bi\{Co(CO)_4\}_4]$[3] and $(RC_5H_4)MoFe(Te_2X)(CO)_5$[4] (X = Br, S_2CNEt_2). Multiple bonding between the group 15 elements is proposed to occur in $E_2[W(CO)_5]_3$ (E = As, Sb, Bi),[5] and an unusual hybrid cluster

Table I. Crystallographic Data for IIa, IIb, and III

	IIa	IIb	III
empirical formula	$BiFe_3CrC_{25}$-$O_{17}H_{20}N$	$SbFe_3CrC_{25}$-$O_{17}H_{20}N$	$Bi_2Fe_2C_{10}H_6O_8$
fw	1034.95	947.72	391.90
cryst syst	triclinic	triclinic	triclinic
space group	$P\bar{1}$ (no. 2)	$P\bar{1}$ (no. 2)	$P\bar{1}$ (no. 2)
b, Å	15.154 (3)	15.108 (5)	8.734 (4)
c, Å	9.791 (1)	9.742 (3)	7.136 (3)
α, deg	107.60 (1)	107.23 (3)	107.02 (4)
β, deg	95.24 (2)	94.61 (2)	108.41 (4)
γ, deg	92.02 (2)	92.37 (1)	79.89 (4)
V, $Å^3$	1727.9 (6)	1710.0 (9)	426.3 (4)
Z	2	2	1
D (calcd), g cm^{-3}	1.99	1.84	3.05
μ, cm^{-1} (Mo Kα)	64.78	24.59	213.07
T(max)/T(min)	1.0/0.69	1.0/0.71	1.0/0.29
wavelength, Å (Mo Kα)		0.71069	
T, °C		23	
residuals: R; R_w	0.045; 0.053	0.042; 0.057	0.041; 0.053

---

(1) (a) Whitmire, K. H. *J. Coord. Chem. B* **1988**, *17*, 95–204. (b) Herrmann, W. A. *Angew. Chem., Int. Ed. Engl.* **1986**, *25*, 56–76.

(2) (a) Herrmann, W. A.; Weichmann, J.; Küsthardt, U.; Schäfer, A.; Hörlein, R.; Hecht, C.; Voss, E.; Serrano, R. *Angew. Chem.* **1983**, *95*, 1019; *Angew. Chem., Int. Ed. Engl.* **1983**, *22*, 979; *Angew. Chem. Suppl.* **1983**, 1543. (b) Herrmann, W. A.; Koumbouris, B.; Schäfer, A.; Zahn, T.; Ziegler, M. L. *Chem. Ber.* **1985**, *118*, 2472. (c) Herrmann, W. A.; Bauer, C.; Weichmann, J. *J. Organomet. Chem.* **1983**, *243*, C21. (d) Rohrmann, J.; Herrmann, W. A.; Herdtweck, E.; Riede, J.; Ziegler, M.; Sergeson, G. *Chem. Ber.* **1986**, *119*, 3544. (e) Huttner, G.; Weber, U.; Sigwarth, B.; Scheidsteger, O.; Lang, H.; Zsolnai, L. *J. Organomet. Chem.* **1985**, *282*, 331. (f) Heberhold, M.; Reiner, D.; Neugebauer, D. *Angew. Chem., Int. Ed. Engl.* **1983**, *22*, 59.

(3) Leigh, J. S.; Whitmire, K. H. *Angew. Chem., Int. Ed. Engl.* **1988**, *27*, 396.

(4) Bogan, L. E., Jr.; Rauchfuss, T. B.; Rheingold, A. L. *Inorg. Chem.* **1985**, *24*, 3720.

0020-1669/89/1328-3164$01.50/0 © 1989 American Chemical Society